VOLUME 120, NUMBER 47
DECEMBER 2, 1998

JOURNAL OF THE AMERICAN CHEMICAL SOCIETY

Developmental Neurobiology Implications from Fabrication and Analysis of Hippocampal Neuronal Networks on Patterned Silane-Modified Surfaces

M. S. Ravenscroft,[†] K. E. Bateman,[†] K. M. Shaffer,[†] H. M. Schessler,[†] D. R. Jung,[†] T. W. Schneider,[†] C. B. Montgomery,[†] T. L. Custer,[†] A. E. Schaffner,[‡] Q. Y. Liu,[‡] Y. X. Li,[‡] J. L. Barker,[‡] and J. J. Hickman*,[†]

Contribution from the Biotechnology Research and Applications Division of Science Applications International Corporation, 6 Taft Court, Rockville, Maryland 20850, and the National Institute of Neurological Disorders and Stroke, National Institutes of Health, Bethesda, Maryland 20892

Received October 22, 1997. Revised Manuscript Received August 24, 1998

Abstract: We have determined the parameters necessary to fabricate *reproducible* neuronal patterns which we are using to begin studying fundamental issues in developmental neurobiology. The addition of a beam homogenizer, as well as a new surface preparation, has enabled the routine production of reproducible, high-resolution (2−20 μm) organosilane patterns. The effects of surface preparation and beam dosage were monitored using X-ray photoelectron spectroscopy (XPS) and proof of patterning is provided by high-resolution imaging XPS. We also report the guidance of neuronal adhesion and neurite outgrowth and the creation of reproducibly defined circuits of embryonic (E18−19) rat hippocampal neurons using these patterned surfaces *in vitro*. We have achieved a >50% rate of pattern formation, and at times the rate approaches 90%. We are using these patterns to address the issue of how geometric pattern cues might be used to affect cell-to-cell communication and we report the preliminary results on the synaptic development of the hippocampal neurons using dual patch-clamp electrophysiology. We monitored neurite outgrowth and the emergence of both spontaneous and evoked synaptic activity for both patterned and unpatterned (control) hippocampal cultures. The results indicate the intriguing possibility that geometry itself may be a modulating or trophic factor for cell development.

Introduction

We have determined parameters for fabricating reproducible neuronal patterns on organosilane surfaces which we are beginning to use to study fundamental developmental questions in neurobiology. X-ray Photoelectron Spectroscopy (XPS) was used in both the high-energy resolution and imaging modes as a diagnostic tool for the optimization of organosilane photolithographic patterns with high-resolution features. The use of a beam homogenizer, a new surface preparation, and optimal laser dosage allowed for the routine production of high-resolution surface patterns. The combination of the optimized patterned surfaces and defined cell culture conditions resulted in high-fidelity neuronal circuits of embryonic rat hippocampal neurons *in vitro*. We show that synaptic development and neurite outgrowth on these neuronal patterns are geometry-dependent and raise the possibility that surface pattern geometry may be a modulating or trophic[1] factor for cell development.

* To whom correspondence should be sent. Current address: Department of Chemistry, The George Washington University, Washington, DC 20052. E-mail: jhickman@gwu.edu.
[†] Biotechnology Research and Applications Division of Science Applications International Corporation.
[‡] National Institute of Neurological Disorders and Stroke.

10.1021/ja973669n CCC: $15.00
Published on Web 11/13/1998

In the work presented here, we impose order on circuits of hippocampal neurons *in vitro* in an attempt to mimic the intrinsic high degree of order of *in vivo* cells in the hippocampus (the region of the brain thought to be responsible for learning and memory functions).[2,3] There are three distinguishable neuronal phenotypes, or subpopulations, of neurons in the mature hippocampus: pyramidal cells, granular cells, and interneurons. Different regions of the hippocampus (*e.g.*, CA1, CA2, and dentate gyrus) contain different proportions of these three subpopulations. Electrophysiological and immunohistochemical studies of mature hippocampal neurons *in situ* and in slice preparations have revealed that the pyramidal and granular cells are excitatory while the interneurons are inhibitory. Both types of signals harmonize in slice preparations to generate long-term changes in fast synaptic transmission, a phenomenon considered to be a cellular correlate of learning. Different pathways that relate to different cognitive functions through this complex cytoarchitecture have been identified.[4] Understanding how the distinct regions of the hippocampus develop and what factors influence the differentiation of premitotic cells into specific cellular phenotypes are some of the challenging issues in developmental neurobiology.

Efforts to unravel the physiological cues underlying the development of neuronal and glial phenotypes and circuit formation *in vivo* have been complemented by rudimentary *in vitro* systems designed to assess the cellular and molecular mechanisms for these processes. Monolayers of embryonic neurons dissociated from the mammalian central nervous system (CNS) and maintained in culture retain cellular and molecular properties reminiscent of those found *in vivo*. Dissociated primary cultures of CNS cells are thus often used for studies designed to elucidate various aspects of neuronal and glial differentiation, including morphogenesis,[5] membrane excitability,[6] cell-to-cell communication,[6] and signal transduction.[7] Some aspects of neuronal differentiation have been studied extensively because they are readily reproducible; however, the experimental results and outcomes may vary due to the complexity and the empirical rationale of the methodology.[5,8,9]

One of the difficulties with presently available protocols for the study of neuronal circuit formation among differentiating neurons and glial cells is that circuits tend to form in an apparently random manner. Greater experimental control would facilitate the study of the pre- and post-synaptic physiological signals occurring during various stages of circuit formation. Etched grooves,[10−12] conventional photoresist technology,[13−15] plasma modification,[16,17] Langmuir−Blodgett films,[18] metal evaporation,[19] photolithography,[20−32] and microcontact printing[33−38] have been utilized to impose order in dissociated cultures by patterning surfaces to control the growth of neurons and other cells. Kleinfeld *et al.*[13] first reliably demonstrated that embryonic mouse spinal cells and perinatal rat cerebellar cells could be confined to grow *in vitro* on patterned organosilane surfaces prepared using conventional photoresist technology. These patterned cerebellar cells developed both electrical excitability and immunoreactivity for neuron-specific enolase which is a marker specific for neurons. The use of deep UV photolithography, which allows for higher resolution patterns, was adopted by some subsequent investigators[20−32] as a more versatile adaptation of the Kleinfeld approach.[13] The use of deep UV photolithography of self-assembled monolayers (SAMs) has been demonstrated to make alternating line patterns of various widths (line-space patterns) to guide the outgrowth of processes from neuroblastoma cells,[20] explanted rat hippocampal cells,[22,26] and human umbilical vein endothelial cells.[22] Corey *et al.*[27] created grid patterns of hippocampal neurons in a low density culture. Healy *et al.*[15] demonstrated the ability to organize bone cells and mineralize tissue *in vitro* on lithographically patterned organosilane surfaces. Our strategy improves on prior work with neurons because we have shown in this paper that SAMs can organize high-resolution neurite outgrowth. Reproducible high-resolution surface templates will facilitate

(1) Hall, Z. W. In *An Introduction to Molecular Neurobiology*; Sinauer Associates, Inc.: Sunderland, MA, 1992, p 27.
(2) Kandel, E. R.; Schwartz, J. H.; Jessell, T. M. In *Principles of Neural Science*, 3rd ed.; Elsevier: New York, 1991.
(3) Skinner, K. J. *Chem. Eng. News* **1991**, Oct. 7, 24−41.
(4) Frotscher, M.; Kugler, P.; Misgeld, U.; Zilles, K. *Adv. Anat. Embryol. Cell Biol.* **1988**, *111*, 1−104.
(5) Banker, G.; Goslin, K. In *Culturing Nerve Cells*; MIT Press: Cambridge, 1991.
(6) Nelson, P. G.; Fields, R. D.; Yu, C.; Neale, E. A. *J. Neurobiol.* **1990**, *21*, 138−156.
(7) Barker, J. L.; Dufy, B.; Harrington, J. W.; Harrison, N. L.; MacDermott, A. B.; MacDonald, J. F.; Owen, D. G.; Vicini, S. *Ann. N.Y. Acad. Sci.* **1987**, *494*, 1−38.
(8) Bottenstein, J. E.; Sato, G. H. In *Cell Culture in the Neurosciences*; Plenum Press: New York, 1985.
(9) Conn, P. M. In *Cell Culture*; Academic Press: San Diego, 1990.
(10) Torimitsu, K.; Kawana, A. *Dev. Brain Res.* **1990**, *51*, 128.
(11) Curtis, A. S. G.; Varde, M. *J. Natl. Cancer Inst.* **1964**, *33*, 15.
(12) Dow, J. A. T.; Clark, P.; Connolly, P.; Curtis, A. S. G.; Wilkinson, C. D. W. *J. Cell Sci. Suppl.* **1987**, *8*, 55.
(13) Kleinfeld, D.; Kahler, K. H.; Hockberger, P. E. *J. Neurosci.* **1988**, *8*, 4098−4120.
(14) Healy, K. E.; Lom, B.; Hockberger, P. E. *Biotechnol. Bioeng.* **1994**, *43*, 792−800.
(15) Healy, K. E.; Thomas, C. H.; Rezania, A.; Kim, J. E.; McKeown, P. J.; Lom, B.; Hockberger, P. E. *Biomaterials*, **1996**, *17*, 195−208.
(16) Vargo, T. G.; Thompson, P. M.; Gerenser, L. J.; Valentini, R. F.; Aebischer, P.; Hook, D. J.; Gardella, J. A. *Langmuir*, **1992**, *8*, 130.
(17) Ranier, J. P.; Bellamkonda, R.; Jacob, J.; Vargo, T. G.; Gardella, J. A.; Aebischer, P. *J. Biomed. Mater. Res.* **1993**, *27*, 917−925.
(18) Ivanova, O. Y.; Margolis, L. B. *Nature* **1973**, *242*, 200.
(19) Letourneau, P. C. *Dev. Biol.* **1978**, *66*, 183.
(20) Dulcey, C. S.; Georger, J. H.; Krauthamer, V.; Stenger, D. A.; Fare, T. L.; Calvert, J. M. *Science* **1991**, *252*, 551.
(21) Georger, J. H. Jr.; Stenger, D. A.; Rudolph, A. S.; Hickman, J. J.; Dulcey, C. S.; Fare, T. L. *Thin Solid Films* **1992**, *210/211*, 716.
(22) Stenger, D. A.; Georger, J. H.; Dulcey, C. S.; Hickman, J. J.; Rudolph, A. S.; Nielson, T. B.; McCort, S.; Calvert, J. M. *J. Am. Chem. Soc.* **1992**, *114*, 8435−8442.
(23) Corey, J. M.; Wheeler, B. C.; Brewer, G. J. *J. Neurosci. Res.* **1991**, *30*, 300−307.
(24) Curtis, A.; Wilkinson, C.; Breckenridge, L. Living Nerve Net. In *Enabling Technologies for Culture in Neural Networks*; Stenger, D., Hickman, J., Eds.; Academic Press: San Deigo, 1994; pp 99−120.
(25) Fromhertz, P.; Schaden, H. *Eur. J. Neurosci.* **1994**, *6*, 1500−1504.
(26) Hickman, J. J.; Bhatia, S. K.; Quong, J. N.; Shoen, P.; Stenger, D. A.; Pike, C.; Cotman, C. W. *J. Vac. Sci. Technol. A*, **1994**, *12*, 607−616.
(27) Corey, J. M.; Wheeler, B. C.; Brewer, G. J. *IEEE Trans. Biomed. Eng.* **1996**, *43*, 944−955.
(28) Kapur, R.; Spargo, B. J.; Chen, M. S.; Calvert, J. M.; Rudolph, A. S. J. *Biomed. Mater. Res.* **1996**, *33*, 205−216.
(29) Potember, R. S.; Pochler, T. O.; Hoffman, R. C.; Speck, K. R. In *Molecular Electronic Devices II*; Carter, F. L., Ed.; Marcel Dekker: New York, 1987.
(30) Stelzle, M.; Wagner, R.; Nisch, W.; Jagermann, W.; Frohlich, R.; Schaldach, M. *Biosens. Bioelectron.* **1997**, *12(8)*, 853−865.
(31) Thomas, C. H.; McFarland, C. D.; Jenkins, M. L.; Rezania, A.; Steele, J. G.; Healy, K. E. *J. Biomed. Mater. Res.* **1997**, *37*, 81−93.
(32) Ito, Y.; Kondo, S.; Chen, G.; Imanishi, Y. *FEBS Lett.* **1997**, *403*, 159−162.
(33) Chen, C. S.; Mrksich, M.; Huang, S.; Whitesides, G. M.; Ingber, D. E. *Science* **1997**, *276*, 1425−1428.
(34) Singhvi, R.; Kumar, A.; Lopez, G. P.; Stephanopoulos, G. N.; Wang, D. I.; Whitesides, G. M.; Ingber, D. E. *Science* **1994**, *264*, 696−698.
(35) Mrksich, M.; Chen, C. S.; Xia, Y.; Dike, L. E.; Ingber, D. E.; Whitesides, G. M. *Proc. Natl. Acad. Sci. U.S.A.* **1996**, *93*, 10775−10778.
(36) Mrksich, M.; Whitesides, G. M. *Annu. Rev. Biophys. Biomed. Struct.* **1996**, *25*, 55−78.
(37) St. John, P. M.; Kam, L.; Turner, S. W.; Craighead, H. G.; Issacson, M.; Turner, J. N.; Shain, W. *J. Neurosci. Methods*, **1997**, *75*, 171−177.
(38) Mrksich, M.; Dike, L. E.; Tien, J.; Ingber, D. E.; Whitesides, G. M. *Exp. Cell Res.* **1997**, *235(2)*, Sept. 15, 305−313.

the study of the factors influencing the formation, maintenance, and modulation of these rudimentary neuronal circuits.

The methodology for using deep UV photolithography to pattern SAMs is relatively new,[20−32] and the critical variables for optimizing this technique are still under investigation. We have previously[26] characterized the mechanisms involved in the photoinitiation process, and we have investigated various combinations of SAMs in an attempt to improve neuronal viability. Only a few molecular combinations (*e.g.*, trimethoxysilylpropyldiethylenetriamine (DETA)/tridecafluoro-1,1,2,2-tetrahydrooctyl-1-dimethylchlorosilane (13F)) were shown to be effective at creating the differential adhesion properties necessary for neuronal patterning. In a recent study, Corey showed that optimized laser conditions produced the best fidelity to a DETA grid pattern, with approximately one-third of the background regions free of connected cells and neurites.[27] However, considerable variation across the surface was noted (*i.e.*, maximal fidelity near the center region of the surface, decreasing with increasing distance from the center). They hypothesized that regional intensity differences in the laser beam profile could be responsible for the variability in pattern fidelity, but lacked analytical methods to prove it.

XPS is an excellent diagnostic tool for characterizing surfaces.[39,40] XPS can be used in the high-energy resolution mode to provide the elemental surface composition and to resolve the oxidation states of individual elements of the surface preparation which allows for the determination of the optimal laser dosage for patterning. XPS can also be used in the imaging mode to provide an element-specific photoelectron image from an organosilane surface which has been patterned. On the basis of the results from our imaging studies, we introduced a beam homogenizer in our process to create uniformity in the energy density of the laser beam and combined this with advances in surface preparation and optimized laser dosages to fabricate high-resolution patterns. The optimized high-resolution circuit patterns successfully guided the neuronal adhesion and neurite outgrowth of embryonic (E) days 18−19 hippocampal neurons in a defined serum-free medium.

Using patch-clamp techniques,[41] we report preliminary results on how geometric cues might be used to affect neurite outgrowth and cell-to-cell communication. We monitored the emergence of both spontaneous and evoked synaptic activity over time in culture for both patterned and unpatterned (control) hippocampal cultures. Our preliminary results presented here indicate that **geometry** itself can serve as a **modulating** or **trophic**[1] factor for cell development.

Materials and Methods

Materials for Film Deposition. Trimethoxysilylpropyldiethylenetriamine (DETA) was purchased from United Chemicals (Bristol, PA). 1H,1H′,2H,2H′-perfluorodecyldimethylchlorosilane (15F) was purchased from PCR, Inc. (Gainesville, FL). Sure-seal toluene was purchased from Aldrich (Milwaukee, WI). The DETA, 15F, and sure-seal toluene were stored in a Labmaster 130 glovebox (MBraun, Innovative Technologies, Inc.) under inert conditions. HPLC-grade toluene, HPLC-grade methanol, reagent-grade hydrochloric acid, and reagent-grade sulfuric acid all from Fisher (Fairlawn, NJ) were used as received.

Surface Preparation. Thomas Red Label micro cover glasses 22 × 22 No. 1 (Thomas Scientific) were cleaned in a series of steps. Ceramic racks (Coors, Inc.) containing the coverslips were soaked in a solution of 50/50 methanol/hydrochloric acid (15 min minimum); rinsed with deionized water (three rinses); soaked in concentrated sulfuric acid (30 min minimum); rinsed with deionized water (three times); boiled in deionized water (30 min minimum); rinsed with acetone (two rinses); and oven dried (15 min, 110 °C).

The cleaned coverslips were then immersed in a 0.1% (v/v) DETA in toluene solution and heated to just below the boiling temperature (30 min). The coverslips were rinsed with HPLC-grade toluene (two rinses), reheated to just below boiling in toluene (30 min), and then oven dried (2 h).

After the DETA-derivatized coverslips were patterned via laser irradiation (see below), the 15F rederivatization or backfill was completed by immersing the rack containing the patterned coverslips in 0.5% (v/v) 15F in toluene solution (1 h). The coverslips were then rinsed with HPLC-grade toluene (three times) and oven dried (15 min minimum).

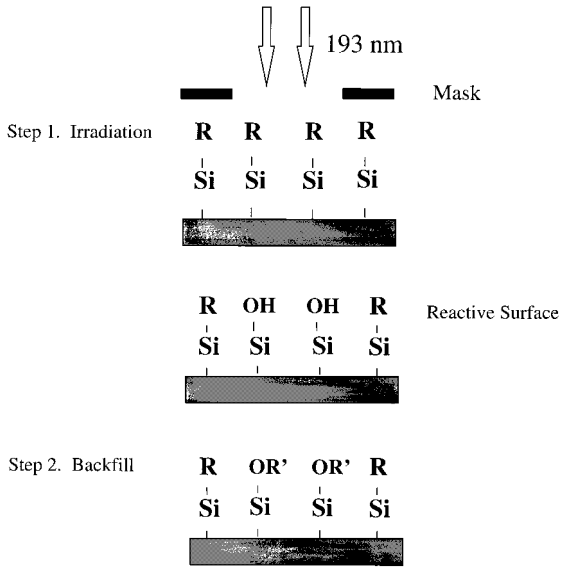

Figure 1. For pattern fabrication, a cytophilic DETA-modified coverslip is irradiated with 193-nm laser light through a photolithographic mask. The resulting reactive surface is then chemically backfilled with the cytophobic silanated 15F. R = $(CH_2)_3$-NH-$(CH_2)_2$-NH-$(CH_2)_2$-NH_2 and R′ = Si-$(CH_3)_2$-$(CH_2)_2$-$(CF_2)_7$-CF_3.

Photolithographic Mask Design. The photolithographic mask used in this work was designed to investigate how geometric cues might be used to control cell growth and affect cell-to-cell communication.[42] The circular pads (20-μm diameter) were designed to adhere a cell body to each of these sites. Both circuit patterns (referred to as RT6 and RT12) had a 7-μm track width, but the overall feature size (length × width) was 520 μm × 270 μm for RT6 and 160 μm × 460 μm for RT12 (see Figures 4 and 7).

Photolithographic Patterning Process. An Ar/F excimer (λ = 193 nm) laser (Lambda LPX210), customized with a beam homogenizer (Exitech, TecOptics, Merrick, NY), was used for all of the experiments. The beam homogenizer has a lens array of 36 elements, designed to achieve a light intensity homogeneity of ±5% over the full aperture. The laser was used in the constant hυ mode (18.4 kV) with a repetition rate in the 20−30 Hz range. An 8 J/cm^2 laser dose was required for the circuit pattern design with a beam area of 2.5 cm^2. For the circuit model, the energy per unit area was 3.0 ± 0.2 mJ/cm^2·shot (as measured by an Astral AA30 power/energy meter) with a burst count of 3000 ± 100 shots, resulting in a pulse time of approximately 2 min. For the line-space pattern, a 10 J/cm^2 laser dose with a burst count of 3700 ± 100 shots resulted in an approximately 3-min pulse time (at the same energy and beam area as reported for the circuit pattern).

For pattern fabrication (Figure 1), a DETA-modified coverslip was irradiated through a photolithographic mask as described above. The UV light served to remove the cytophilic DETA in the exposed areas,

(39) Briggs, M. P.; Seah, M. P. In *Practical Surface Analysis by Auger and X-ray Photoelectron Spectroscopy*; John Wiley & Sons: New York, 1983 and 1992.

(40) Scofield, J. H. *J. Electron Spectrosc. Relat. Phenom.* **1976**, *8*, 129.

(41) Neher, E.; Sakmann, B. *Sci. Am.* **1992**, 44−51.

(42) Assistance from Stenger, D. A., Center for Bio/Molecular Science and Engineering, Code 6910, Naval Research Laboratory, Washington, DC 20375.

creating a reactive surface which was then backfilled with the cytophobic silane 15F.

XPS Characterization. VG Scientific XPS Model ESCALAB 220i-XL is capable of both real-time imaging and high-energy resolution spectroscopy. The XPS was used in both modes for this work. Chemical imaging via XPS has been previously reported.[39,40] In the high-energy resolution mode, the takeoff angle was 35° and the spectra were normalized to the Si 2p peak of the substrate. To image patterned DETA, the surface was first modified with a Pd catalyst as described by Dressick *et al.*[43,44] for selective electroless Ni deposition. In this manner, we can increase the signal from the nitrogen (N 1s) because the Pd complexes to the amine groups of the DETA. If it was desired, we could further react the Pd with a Ni bath to produce both an optical and a chemical image of the pattern. With the VG instrument, spatial resolution of a few micrometers is attainable for our patterned surfaces.

Contact Angle Measurements. Using the sessile drop technique,[45−47] a drop of deionized water was dispensed at the silanated surface via the microsyringe of an NRL contact angle goniometer model 100-00 (Ramé-Hart, Inc.) to measure the surface wettability. Both the advancing and receding contact angles were measured for each surface.

Cell Culture Conditions. Hippocampal neurons were isolated from E18-E19 Sprague−Dawley rat (Taconic Farms, Germantown, NY) embryos by papain dissociation (2 units/mL, Worthington Biochemical Corp., Lakewood, NJ). After dissociation, the cells were centrifuged, resuspended, layered over a step gradient, centrifuged through the gradient to remove debris, and then resuspended in the culturing media.[48] The cells were counted using a hemacytometer and plated at a density of optimum 56×10^4 cells per 22 mm × 22 mm coverslip. This was the minimum density that enabled cell survival long enough for electrophysiological measurements. Higher plating densities could have increased survivability, but the aggregation increased as the density increased which decreased the pattern fidelity results accordingly. The cells were cultured in a serum-free Neurobasal medium (Life Technologies, Gibco BRL, Grand Island, NY) supplemented with B27 (Life Technologies, Gibco BRL, Grand Island, NY), glutamine (0.5 mM, Life Technologies, Gibco BRL, Grand Island, NY), and glutamate (25 μM, >99% TLC, Sigma Chemical, St. Louis, MO)[49] at 37 °C and 5% CO_2.[50] At days 2, 4, 8, (and subsequent multiples of 4) *in vitro*, 50% of the media was removed and replaced with Neurobasal medium supplemented with B-27 and glutamine (*i.e.*, without the glutamate). The removal of the glutamate was necessary to prevent neurotoxicity.[49]

We report statistical averages for pattern fidelity. Since the mask allows for 100 circuit RT6 patterns to be created per coverslip, cell pattern fidelity was tabulated as *x*/100 positive circuit patterns per coverslip. The number of cells attached at the circular somal sites were tabulated and averaged. We used an inverted microscope (Olympus CK2, Opelco, Sterling, VA) adapted with a digital CCD camera (3CCD, Dage-MTI, Inc., Michigan City, IN) and an Intel Pentium notebook computer (Travel Mate, Texas Instruments) to acquire and store pattern images and Image-Pro Plus software (Cybernetics) to tabulate the average number of neurites per cell and the average neurite length.

Immunocytochemistry Procedure. The cells were preserved in 4% paraformaldehyde in Dulbecco's phosphate buffered saline (D-PBS). After the cells were exposed for 30 min to the paraformaldehyde fixative, they were rinsed with D-PBS (Quality Biologicals, Inc.) and refrigerated. For immunostaining, the fixed plates were incubated with mouse monoclonal anti-MAP-2 (1:300, Sigma) overnight at 4 °C. After a D-PBS rinse, the cells were incubated in FITC-conjugated donkey anti-mouse IgG (1:50, Jackson Immunological Research) for 45 min at room temperature. The labeled cells were examined on an epifluorescence microscope (Zeiss) with a water immersion 25× objective.

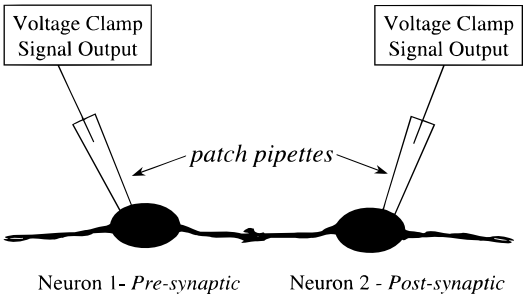

Figure 2. Schematic illustration of the experimental arrangement for dual patch-clamp recording. Both neurons are voltage clamped, and the current signal is recorded for both spontaneous (single neuron) occurrences and evoked (pre-synaptic neuron to post-synaptic neuron) responses.

Electrophysiology Experiments. Whole cell patch-clamp techniques were carried out on pairs of patterned neurons to record functional connections. Dual patch-clamp recordings were carried out using current- and/or voltage-clamp configurations. We looked for evidence of synaptic-like transient signals that were either **spontaneous** occurrences or **evoked** responses. Spontaneous occurrences were the natural electrical activity of cells during development that appear random in nature. In the case of evoked responses, a voltage was applied to one (pre-synaptic) cell and a current signal from the second (post-synaptic) cell is recorded (Figure 2). The electrophysiology setup consisted of a L/M EPC-7 patch-clamp system (LIST-Medical), an inverted microscope (Zeiss), a model 7313 oscilloscope (Tektronix, Inc.) with simultaneous readout from both a CRC VR-100B digital recorder (INSTRUTECH Corp.) and a Brush 260 chart recorder (Gould). The cells were sealed with glass patch pipets filled with a buffered intracellular Ca^{2+}-ATP solution. The extracellular solution was Tyrode's solution.[5] Initial membrane potentials were consistently measured at −80mV.

Results

Our report on the fabrication of the cell patterns proceeds through several steps from chemistry and photolithography to cell culture and finally electrophysiological characterization of cell function.

A. Characterization of Unpatterned Aminosilane Surface. It was reported previously[51] that DETA promotes the adhesion and growth of hippocampal neurons. Cell culture on an unpatterned cytophilic DETA surface resulted in hippocampal neurons which were phase dark, indicating strong adherence, with extended neurites (Figure 3a). High-resolution XPS for the DETA surface preparation yielded a nitrogen (N 1s) intensity of 3600 ± 900 counts when normalized to a silicon (Si 2p) peak area of 5000. This compares to our previously reported methanol DETA surface preparation, which yielded a nitrogen (N 1s) intensity of 1300 ± 300 counts when normalized to a Si 2p peak area of 5000.[26] The advancing and receding contact angles for the new DETA preparation with their standard deviations were $\theta_{adv} = 42° \pm 3°$ and $\theta_{rec} = 6° \pm 5°$, respectively.

B. Characterization of Unpatterned Fluorinated Silane Surface. In contrast to DETA, 15F (much like the previously reported 13F)[26] impedes neuronal adhesion and neurite outgrowth. The hippocampal neurons become phase bright, indicating poor adhesion to the surface, with the cell bodies appearing clumped and the neurites fasiculated (Figure 3b).

(43) Dressick, W. J.; Dulcey, C. S.; Georger, J. H., Jr.; Calabrese, G. S.; Calvert, J. M. *J. Electrochem. Soc.* **1994**, *141*, No. 1, 210-220.
(44) Kapur, R.; Spargo, B. J.; Chen, M. S.; Calvert, J. M.; Rudolph, A. S. *J. Biomed. Mater. Res.* **1996**, *33: 4*, 205−16.
(45) Johnson Jr., R. E.; Dettre, R. H. *Surf. Colloid Sci.* **1969**, *2*, 85.
(46) Neumann, A. W.; Good, R. J. *Surf. Colloid Sci.* **1979**, *11*, 31.
(47) Drelich, J.; Wilbur, J. L.; Miller, J. D.; Whitesides, G. M. *Langmuir* **1996**, *12*, 1913−1922.
(48) Schaffner, A. E.; Barker, J. L.; Stenger, D. A.; Hickman, J. J. *J. Neurosci. Methods* **1995**, *62: 1−2*, 111−119.
(49) Brewer, G. J.; Torricelli, J. R.; Evege, E. K.; Price, P. J. *J. Neurosci. Res.* **1993**, *35*, 567−576.
(50) Brewer, G. J. and Cotman, C. W. *Brain Res.* **1989**, *494*, 65−74.
(51) Stenger, D. A.; Pike, C. J.; Hickman, J. J.; Cotman, C. W. *Brain Res.* **1993**, *630*, 136−147.

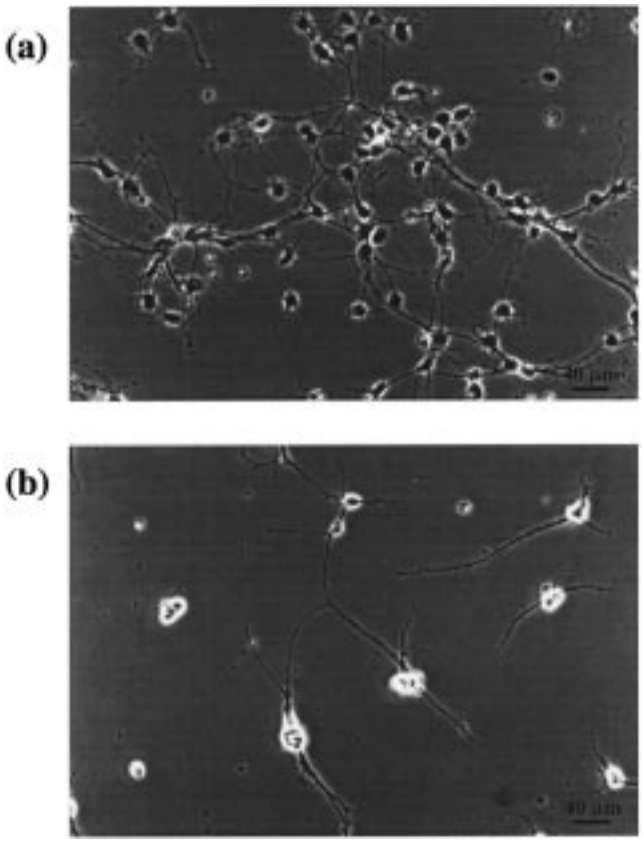

Figure 3. Day 4 *in vitro* hippocampal neurons at 20× magnification plated onto unpatterned (a) DETA-coated glass coverslip where the cells appear phase dark and (b) 15F-coated glass coverslip where the cells appear phase bright with fasiculated (bundled) neurites.

High-resolution XPS for the 15F surface preparation yields a fluorine (F 1s) intensity of 14 200 ± 400 counts when normalized to a Si 2p peak of 5000. This compares to our previous methanol 13F surface preparation, which yielded a fluorine (F 1s) intensity of 8230 ± 3000 counts when normalized to a Si 2p peak of 5000.[26] The advancing and receding contact angles for 15F with their standard deviations were $\theta_{adv} = 90 \pm 1°$ and $\theta_{rec} = 79 \pm 5°$.

C. Fabrication and Analysis of Circuit Patterns by XPS. We previously used deep UV laser patterning to reproducibly create line-space patterns.[26] However, when we tried to fabricate the more complex, higher resolution pattern designs, we were unable to routinely produce high quality patterns as evidenced by the optical images provided from Pd/Ni metallization and by poor cell fidelity to the patterns. The nonuniform energy density distribution of the laser beam at the substrate surface[27] is shown in the optical photo in Figure 4a. We therefore utilized a beam homogenizer to deliver a top-hat energy profile of the laser beam at the substrate surface, resulting in uniform patterning as shown in the optical photo in Figure 4b. Patterns fabricated in this way yielded more uniform images in XPS and greater fidelity of cells to the patterns.

After incorporation of the beam homogenizer, the best laser dosage for the circuit pattern design was determined. An optimal laser dose must be high enough to remove the aminosilane (DETA) during the patterning process but low enough to prevent narrowing of the line widths and ablation of the right-angled features of the circuit design as seen in Figure 5. XPS analysis showed that a 5 J/cm^2 laser dose was necessary to remove 50% of the amine (N 1s signal) from the surface, and a 15 J/cm^2 dose was required to clear the amine from the surface. The best circuit patterns were found with a dose of 8 J/cm^2, as shown by imaging XPS in Figure 6. We chose the DETA surface for pattern formation because previous work[26] had shown the dosage required to remove the 13F was greater than 60 J/cm^2.

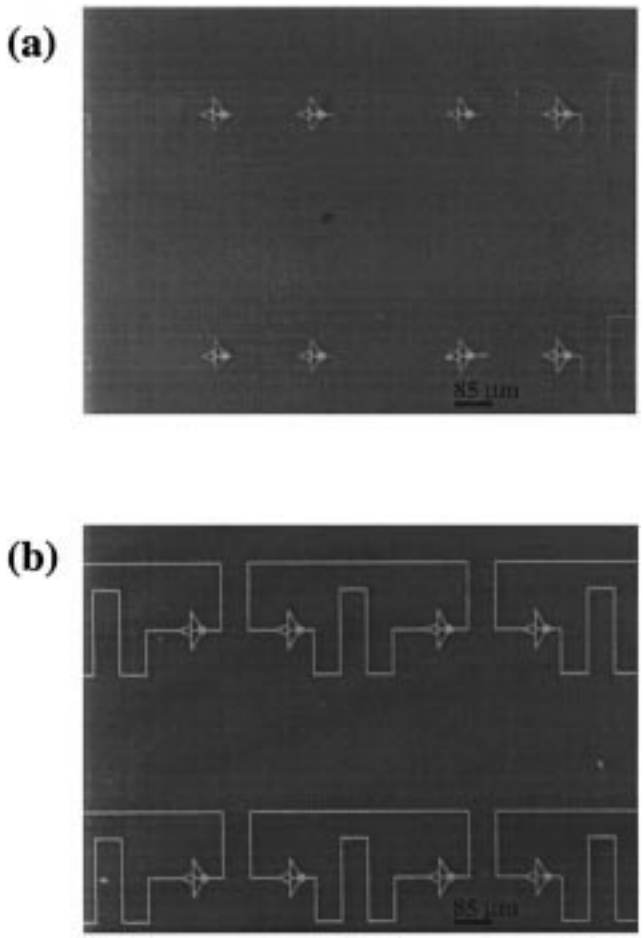

Figure 4. Optical images of Pd/Ni-metallized RT6 circuit images prepared (a) without the beam homogenizer and (b) with the beam homogenizer.

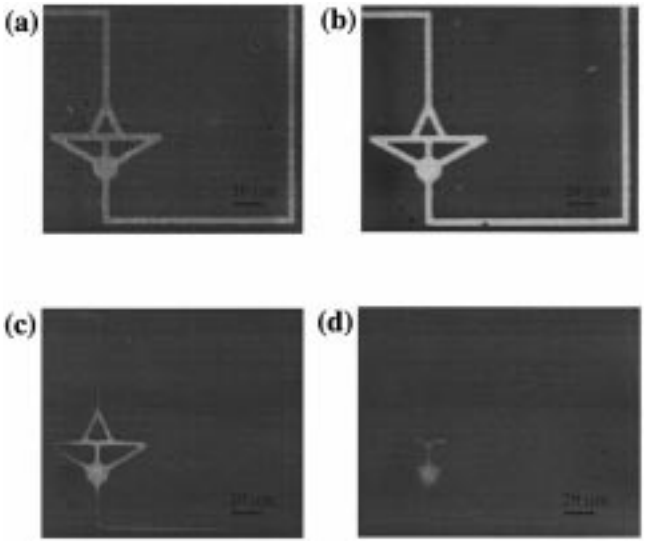

Figure 5. Optical images (20×) of Pd/Ni-metallized RT6 circuit at laser dosages of (a) 5 J/cm^2, (b) 8 J/cm^2, (c) 10 J/cm^2, and (d) 15 J/cm^2.

D. Characterization of Cells Adhered to Circuits.

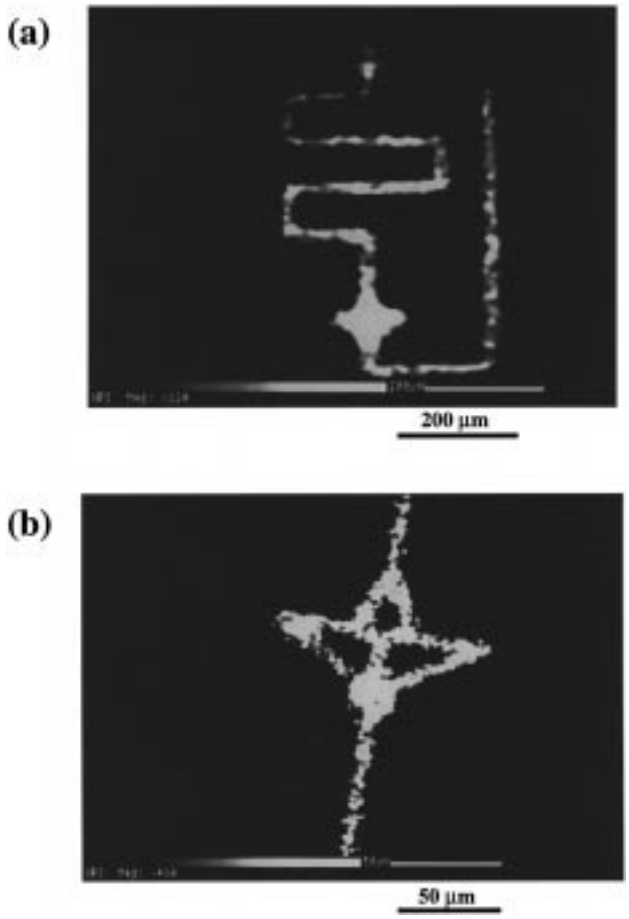

Figure 6. XPS images of (a) a circuit RT6 pattern and (b) a circular somal adhesion site. In both cases, the patterns are metallized with Pd/Ni, and the Ni 3p signal is imaged.

1. Cell Adhesion to Individual Circuit Patterns. The ability to control surface composition coupled with the appropriate media conditions has been shown to be effective in influencing neuronal development *in vitro*.[48] In our experiments, the E18−19 hippocampal neurons were plated in the B-27-supplemented medium and circuit patterns were observed as early as 1 h after cell plating. Staining with MAP-2, a selective marker for developing hippocampal dendrites, at days 2 and 7 confirmed that the cells were neuronal.[52] Both the circuit (Figure 7) and line-space patterns (Figure 8a) were successful in controlling the cell adhesion and neurite outgrowth. Cell fidelity was monitored using the optimized RT6 circuits ($n = 400$) with their somal adhesion sites ($n = 800$) at each time interval *in vitro*. Two hours after plating, 23 ± 12% fidelity to individual patterns and 17 ± 6% fidelity to somal sites were observed. Cell pattern fidelity peaked on day 1 with 75 ± 15% pattern fidelity and 30 ± 5% somal fidelity. On day 2, the pattern and somal fidelity were 68 ± 6% and 26 ± 2% respectively. Although the cells continued to be viable, the pattern fidelity declined through day 7 when 1% pattern fidelity remained. Cell pattern fidelity for the line-space patterns was >90% on day 1 and declined through day 14.

2. Increased Variance in Cell Morphology on Circuits. The cell morphology showed differences between patterned and unpatterned cells at the early time points. On days 1 and 2, the cells on the unpatterned DETA surfaces were phase dark with extensive growth cones with short intertwined neurites mostly confined to the growth cone area (Figure 8b). At the same time points, the cells on the patterned surfaces (Figures 7 and 8a) lacked the extensive growth cones, but a greater variance

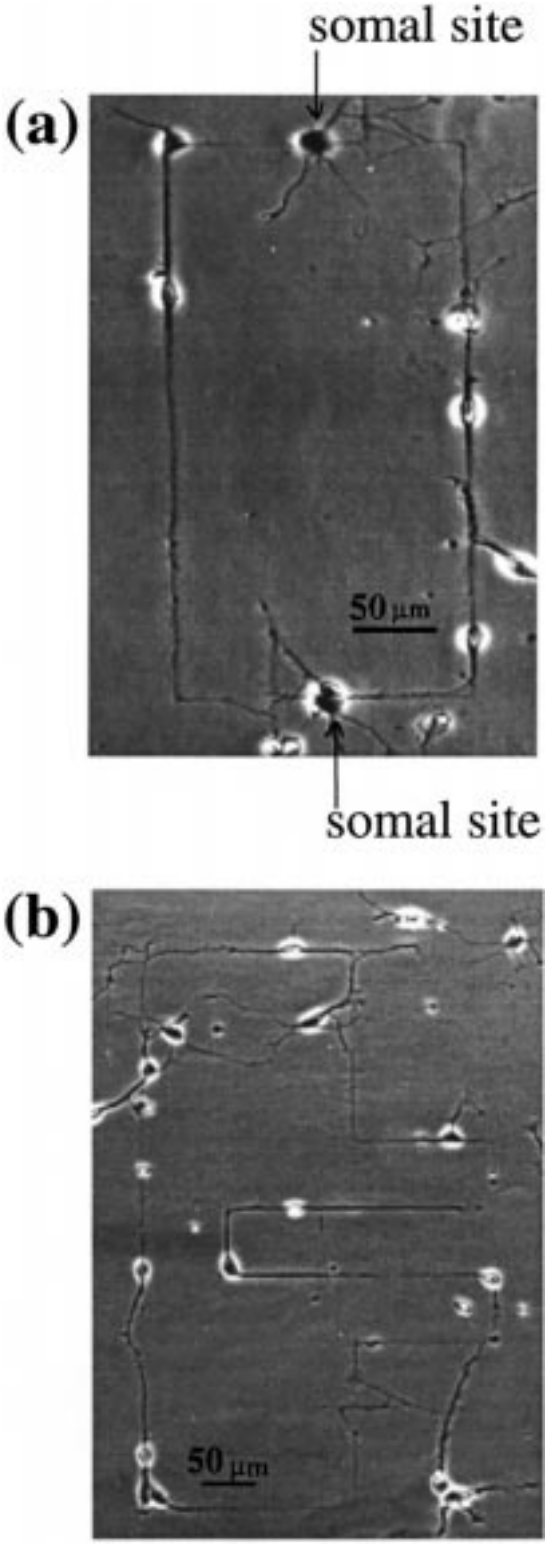

Figure 7. Photograph (20×) of patterns of day 2 *in vitro* hippocampal neurons on (a) the circuit RT12 mask feature and (b) the circuit RT6 mask feature.

in neurite length was observed. The average neurite length and number of primary neurites per cell on the RT6 circuits on day 2 was 59.3 ± 35.3 μm and 2 ± 1 μm, respectively. For the line-space patterns, the average neurite length and number of neurites per cell on day 2 was 47.6 ± 25.5 μm and 2 ± 1 μm, respectively. For the unpatterned DETA-modified surfaces, the average neurite length and number of neurites per cell on day 2 was 31.0 ± 14.3 μm and 2 ± 1 μm, respectively. This

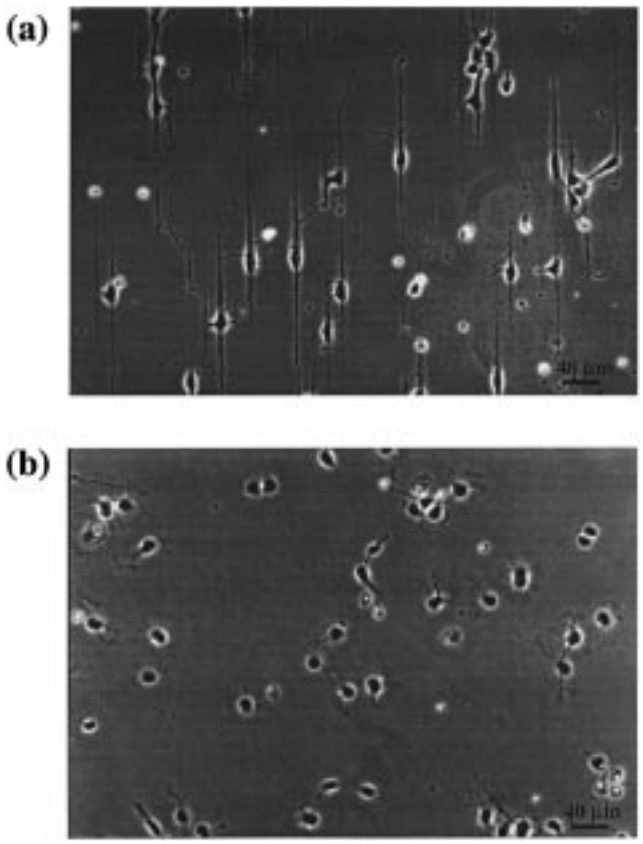

Figure 8. Day 2 *in vitro* hippocampal neurons (20×) plated onto (a) a DETA/15F line-space pattern and (b) unpatterned DETA.

increase in variability of neurite outgrowth on the patterned surfaces vs the unpatterned surfaces is consistent with and correlates with the morphological differences.

3. Electrophysiology of Circuits. An indication of synaptic activity can be shown with neurotransmitters, which migrate across the synaptic cleft to the dendrites of the post-synaptic cell after release from axonal endings and are necessary for functional synaptic activity.[5] In the *adult* mammalian central nervous system, gamma-aminobutyric acid (GABA) is the major inhibitory neurotransmitter.[53−56] In immature rats, GABA depolarizes hippocampal neurons and increases intracellular [Ca^{2+}] and is generally considered excitatory.[57] The switch from excitatory to inhibitory function for GABA comes early in postnatal development, but in either case the presence of GABA in embryonic culture is indicative of synaptic development. The other major neurotransmitter found in the *adult* mammalian cells is glutamate, which is excitatory. GABA is produced from glutamate in the presence of glutamate decarboxylase (GAD).[54] Recently, Dupuy and Houser[58] discovered that GAD-67- and GAD-65-containing neurons could be observed as early as E17−18 in the rat hippocampus, indicating the presence of both neurotransmitters in early embryonic development.

The dual patch-clamp technique (described in the Experimental Section) was used to look for both spontaneous and evoked synaptic activity over the time course of the hippocampal cell development on both the patterned and unpatterned silanated substrates. In the B27-supplemented Neurobasal serum-free defined medium,[49] the GABA[53,54,59,60] initiated synaptic signals develop over time in culture. Recordings during the first 6 days after cell plating for **both** the unpatterned and patterned surfaces gave no evidence of either spontaneous or evoked synaptic activity *in vitro*. By day 7 or 8, both spontaneous and unidirectional evoked synaptic signals for the **unpatterned** DETA surface were recorded (Figure 9a). However, only spontaneous activity (*i.e.*, a lack of evoked response) was observed for the **patterned** (line-space and circuit patterns) surfaces at day 7 or 8 (Figure 9b). By day 12, the cells on the line-space patterned surface displayed **both** spontaneous and unidirectional evoked synaptic signals (Figure 10b). The day 12 cells on the unpatterned DETA surface displayed both spontaneous activity and a preference for evoked signals in one direction (Figure 10a). Figures 9 and 10 clearly show that the nonevoked activity is spontaneous synaptic activity and not single-ion channel openings or noise due to the characteristic fast rise and slow decay of these signals. If this activity were due to single ion channels, there would be an "all or nothing" response, and signals due to electrical noise are generally symmetrical about the baseline. The longevity of the circuit patterns was about a week; therefore, we were unable to provide the day 12 data for this particular pattern for comparison. However, it is interesting that the same trend in signal emergence is observed through the entire first week for the cells on both the line-space and circuit patterned surfaces.

Discussion

Using patterned artificial surfaces, we have achieved a high degree of neuronal fidelity to patterned circuits as determined by the percentage of cell circuit patterns formed on the high-resolution DETA/15F templates. In a defined medium, the neurons were able to reproduce some fundamental developmental processes under the conditions of geometric constraint on the circuit patterns. The steps we have outlined here, combined with appropriate surface analysis, should now allow a large number of researchers access to this methodology. We believe this is the single most important result in this paper.

The achievement of reproducible patterns has allowed us to begin monitoring the effects of patterns in statistically significant numbers. The lack of extensive growth cones for the patterned neurons and a greater variance in neurite length indicate that geometric constraint affected the cell morphology at early time points. Specifically, when the neurons were given fewer degrees of freedom for neurite extension, a larger variance in neurite length was consistently observed. Mennerick *et al.*[55] recently suggested that postnatal rat hippocampal neurons that constrained microisland neurons elaborated less extensive neuritic arborizations than neurons cultured randomly. Collectively, these results imply that geometry is a subtle contributing factor for earlier, directed growth of neurites.

Despite the earlier accelerated growth for hippocampal neurons on patterned surfaces, we observed greater longevity on the unpatterned DETA surfaces. In fact, the order of hippocampal neuron longevity for the various surfaces was consistently as follows: DETA, unpatterned (longevity of 1 month) > DETA/15F, line-space pattern (longevity of 2 weeks) > DETA/15F, circuit pattern (longevity of 1 week). For the patterned cells, the term longevity is meant to imply the length

(52) Dotti, C. G.; Sullivan, C. A.; Banker, G. A. *J. Neurosci.* **1988**, *8*, 1454−68.
(53) Steit, P.; Thompson, S. M.; Gähwiler, B. H. *Eur. J. Neurosci.* **1989**, *1*, 603−615.
(54) Hoch, D. B.; Dingledine, R. *Dev. Brain Res.* **1986**, *25*, 53−64.
(55) Mennerick, S.; Que, J.; Benz, A.; Zorumski, C. F. *J. Neurophysiol.* **1995**, *73*, 320−332.
(56) Bayer, S. A. *J. Comp. Neurol.* **1980**, *190*, 115−134.
(57) Berninger, B.; Marty, S.; Zafra, F.; de Penha Berzaghi, M.; Thoenen, H.; Lindholm, D. *Development* **1995**, *121*, 2327−2335.
(58) Dupuy, S. T.; Houser, C. R. *J. Neurosci.* **1996**, *16*, 6919−6932.
(59) Ozawa, S.; Yuzaki, M. *Neurosci. Res.* **1984**, *1*, 275−293.
(60) Segal, M.; Barker, J. L. *J. Neurophysiol.* **1984**, *52*, 469−487.

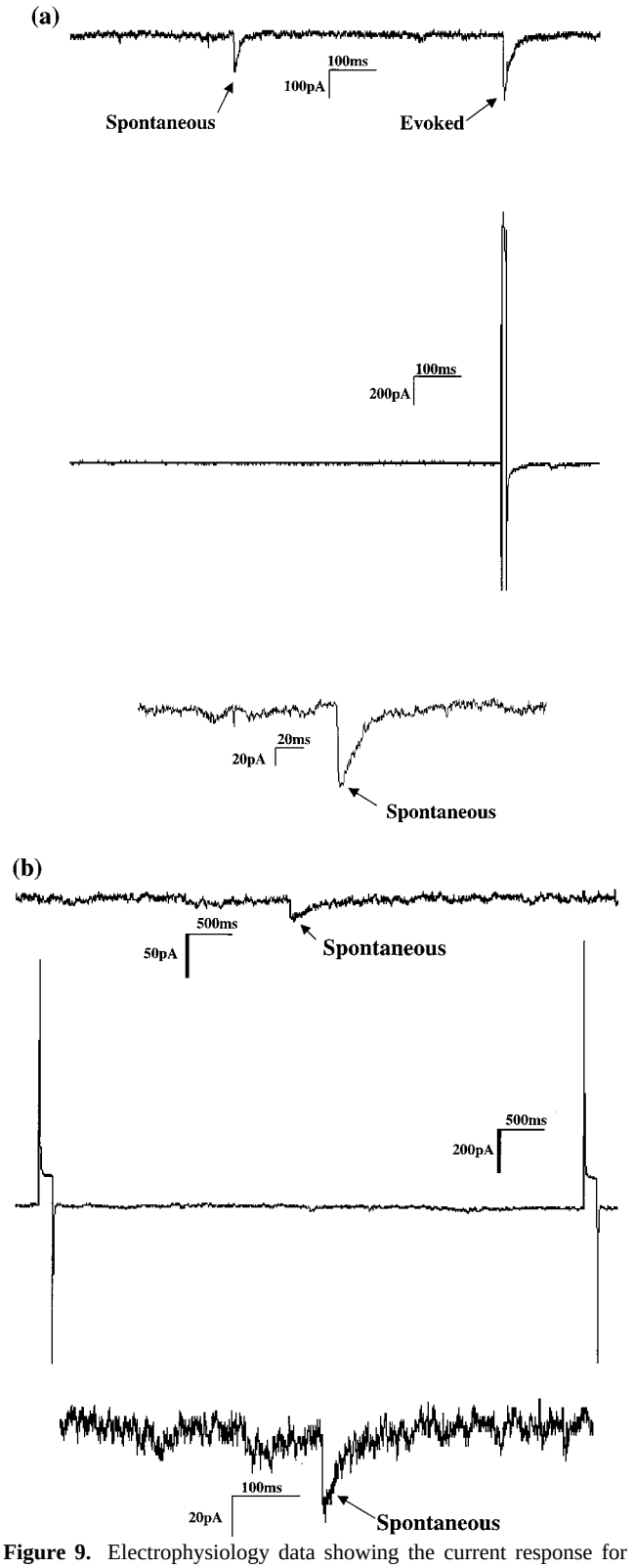

Figure 9. Electrophysiology data showing the current response for day 8 *in vitro* hippocampal neurons on (a) an unpatterned DETA-modified surface displaying both spontaneous and evoked activity, and (b) a DETA/15F circuit patterned surface displaying only spontaneous activity. In both cases, the top trace represents the current response of the post-synaptic neuron, the middle trace represents the stimulation current applied to the pre-synaptic neuron, and the bottom trace represents an enlargement of a spontaneous current signal from the top trace (post-synaptic neuron).

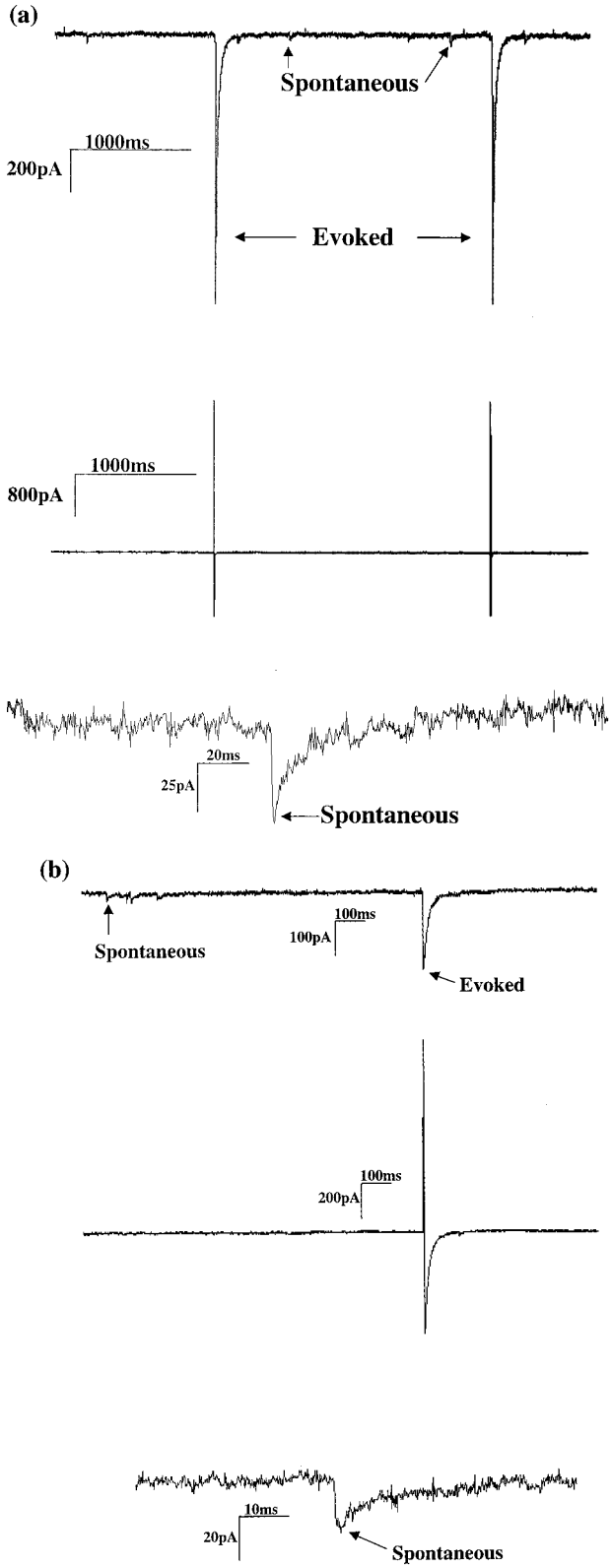

Figure 10. Electrophysiology data showing the current response for day 12 *in vitro* hippocampal neurons displaying both spontaneous and evoked activity on (a) an unpatterned DETA-modified surface and (b) a DETA/15F line-space patterned surface. In both cases, the top trace represents the current response of the post-synaptic neuron, the middle trace represents the stimulation current applied to the pre-synaptic neuron, and the bottom trace represents an enlargement of a spontaneous current signal from the top trace (post-synaptic neuron).

of pattern recognition, not cell viability, since the cells often continued to live long after the neurites had overgrown the pattern feature. We previously reported the use of XPS to monitor the deposition of protein in serum-free media at the

artificial surface−cell interface.[26,48] We hypothesize in the present case that the protein deposition may be obscuring the patterns with time. We further hypothesize that the difference in the longevity of pattern recognition between the line-space and circuit patterns may be due to cell density factors. As the pattern features get smaller, the number of healthy neurons decreases since more cytophobic surface is present. Diffusable factors from the cells have been shown to affect longevity, and the concentration of these factors decreases as cell density decreases, lowering survival times. We will investigate these potential factors with new mask designs for further optimization in future work.

Synaptic development is also of keen interest to our group, and exploring this fundamental developmental process was the area in which we chose to demonstrate the utility of the pattern reproducibility. *In vivo*, the rat hippocampus is recognizable prenatally on E16. The region is postulated to develop on E15 with the connection of two primordia in the telencephalon. The most rapid growth occurs between E16 and E17 with a volumetric increase of 1900%. The embryonic birth date is E22, but the volumetric expansion of the hippocampus continues through postnatal (PN) day 21.[58] Thus, in the present study, we are starting with very immature hippocampal neurons that have not yet established connections. This allows us to study synaptic development from the initial periods of hippocampal development.

In the present work, we used dual patch-clamp electrophysiology to monitor the emergence of synaptic activity *in vitro* for hippocampal neurons dissociated with papain from E18−19 rats. We wanted to determine if patterned artificial surfaces could influence the synaptic development *in vitro*. In all of the evoked synaptic activity (responses to electric pulses through the patch clamp), we observed physiological responses of GABAergic origin as determined by the electrophysiological signature. On the unpatterned DETA-modified surfaces, we observed both spontaneous and evoked activity by day 7 or 8. On the patterned surfaces (*i.e.*, line-space and circuit designs) we observed only spontaneous currents by day 7 or 8 with the evoked activity being delayed until day 12 for the patterned (line-space) surface. This delayed onset of evoked activity occurred despite the earlier accelerated growth and visible formation of overlapping connections for the patterned axons and dendrites. In addition, the evoked synapses always showed a unidirectional preference. Although a direct correlation between *in vitro* cultures and slice cultures cannot yet be made, it is well established that in slice preparations glutamatergic synaptic activity is unidirectional from CA1 to CA3 neurons.[61] We conclude that the geometric control by patterning is a modulating or trophic[1] factor for both the cell morphology and the neuronal synaptic development. Our goal now is to begin developing this new tool to *control* synaptic activity for *in vitro* model systems and to extend this preliminary example of the utility of the reproducible surface chemistry to study the effect of growth factors and other pharmacological agents using these reproducible minimalistic neuronal circuits.

Conclusions

Using XPS, a new surface preparation, optical microscopy, and a beam homogenizer for a more uniform deep UV photolithography, we have achieved uniform, routine, high-resolution photolithographic circuit patterns on artificial surfaces. We have achieved a >50% rate of pattern formation and at times the rate approached 90% for the optimized high-resolution circuit patterns using specific media conditions. With the defined neuronal connections created by the patterns, we were able to begin exploring the fundamental issue of how geometry affects both cell morphology and synaptic development *in vitro*. We conclude that geometry itself may be a modulating or trophic[1] factor that is the cause of greater variance in neurite outgrowth at early time points and delayed synaptic development for the patterned cells until later time points.

We plan to use our high fidelity, high-resolution circuit patterns to study many aspects of neuronal development in a controlled manner. New mask designs will now be used to control the parameters in our *in vitro* system and to investigate how varying geometry affects neuronal development. We believe a combination of controlled cell density and patterns with co-cultures of glial and neuronal cells without their being intermixed will eventually enable culture for periods of time observed by Banker[5] of up to six months. We will address the issue of long-term fidelity by looking at negative surfaces that are repulsive to cell overgrowth as well as address the issue of endpoint development to encourage the transformation of cells to fixed behavior.

Acknowledgment. We thank the NRL for permitting us to use their laser facilities and Dr. Wu Ma for his help with antibody staining. This work was funded by the Department of Energy grant DE-FG02-96ER14588 and SAIC internal research and development funds. The beam homogenizer was purchased with funds from the Office of Naval Research.

JA973669N

(61) Sik, A.; Ylinen, A.; Penttonen, M.; Buzsaki, G. *Science* **1982**, *265*, 1722−1724.